SNOW COVER AND GLACIERS

THE STRUCTURE OF THE UPPER PART OF THE GLACIER IN THE AREA OF A SNOW-RUNWAY OF MIRNY STATION, EAST ANTARCTICA (BASED ON THE DATA COLLECTED IN 2014/15 FIELD SEASON)

S.V. Popov[1], S.P. Polyakov[2], S.S. Pryakhin[2], V.L. Mart'yanov[2], V.V. Lukin[2]

[1] *Polar Marine Geosurvey Expedition,*
24, Pobeda str., St. Petersburg, Lomonosov, 198412, Russia
[2] *Arctic and Antarctic Research Institute,*
38, Beringa str., St. Petersburg, 199397, Russia; spopov67@yandex.ru

The main results of GPR sounding and ice core sampling carried out in the area of the Russian Mirny Station area during the austral summer field season of 60th Russian Antarctic Expedition (2014/15) are presented. The GPR data were collected at the frequencies of 270 MHz and 900 MHz. The total length of the profiles was 20 km. Five ice cores about 7 m long were selected. The upper part of the glacier was found to consist of a snow-firn layer and meteoric ice underneath. The effective permittivity of the media were determined to be 2.13 and 3.0, accordingly. The snow-firn layer thickness varied between zero ('blue ice') and approximately 40 m.

East Antarctica, Mirny Station, GPR sounding, ice core sampling, diffracted waves, snow-firn layer

---

INTRODUCTION

The first Soviet research station in the Antarctic, *Mirny*, was opened on February 13, 1956 on the coast of the Davis Sea. It was there where a base site of the logistic and scientific traverses has existed for over half a century, to explore the continent's internal regions. From there the explorers went off to open the *Pionerskaya, Komsomolskaya, Vostok* Antarctica research stations and to raise the state flag of the USSR on the Pole of Inaccessibility. It was from *Mirny* that the basic procurement had been carried out for the *Vostok* station for over fifty years. Along with the solution of logistical tasks, the traverses performed a large number of research programs, among which glaciological and geophysical studies occupied an important place [*The first... expedition, 1959; Treshnikov, 1963; Savatyugin and Preobrazhenskaya, 1999; Lukin et al., 2006*].

Since movement of the transport base to the *Progress* station (the first experimental Progress – Vostok logistic traverse took place in the field season of the 53th Russian Antarctic expedition (RAE), 2007/08), the *Mirny* station has not lost its strategic significance. It continues to be an important logistical hub, as it allows connection of the intracontinental air routes of East Antarctica [*Polyakov et al., 2015*]. However, for the base effectively to function as a hub,

the snow runway, which used to exist there, has to be restored. For this purpose, during the austral summer field season of the 59th RAE (2013/14), S.V. Volf conducted recognizance works, which included GPR sounding and fixing of glaciological landmarks to determine the flow velocity of the glacier in this region. In the season of the 60th RAE, in the period of January 10–21, 2015, large-scale geophysical survey was conducted. It was intended to study the upper part of the glacier and, in particular, to reveal crevasses of significant sizes. The works included: 1) aerial photography, 2) GPR soundings, 3) ice core sampling and 4) glacier monitoring [*Polyakov et al., 2015; Popov et al., 2015; Pryakhin et al., 2015*]. The location chart is depicted in Fig. 1. The size of the paper does not allow the authors to describe all the aspects of the works conducted; therefore, only part of the results obtained is presented.

METHODOLOGY AND EQUIPMENT

Aerial photography was performed on January 11, 2015 onboard a helicopter Ka-32 (board number RA-31021) from the relative altitude of 1500 m. The works were conducted over the territory of 3.5 × 3.5 km, covering 14 routes totaling 52.5 km with the inter-route distance of 280 m. During the survey,
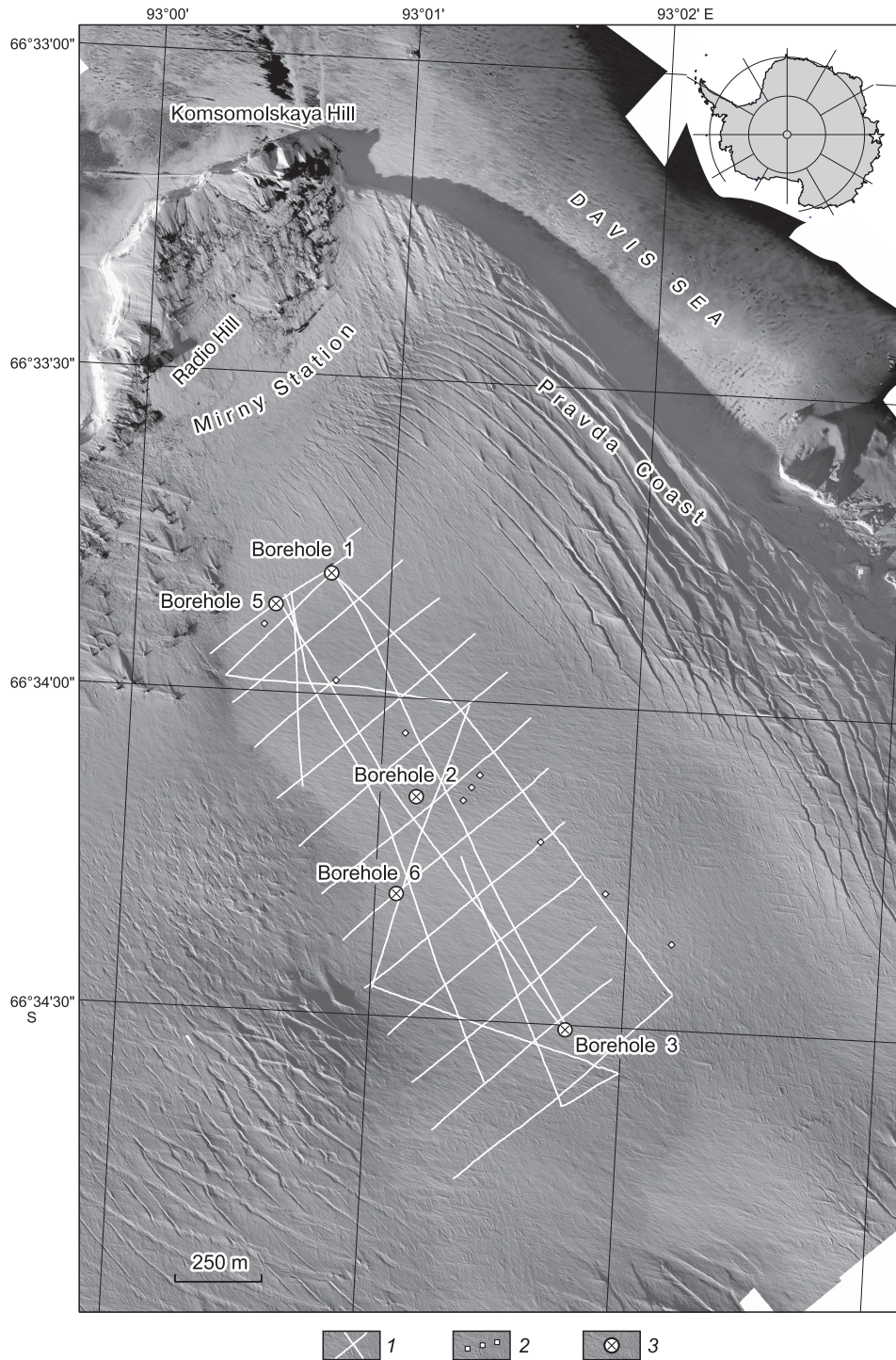
Fig. 1. Glaciological and geophysical works:

1 – GPR routes; *2* – glaciological landmarks for determining the glacier flow velocity; *3* – core drilling points.

a digital camera Canon 650D with the Canon EF 40 mm 1:2.8 STM lens was used. In total, 219 photo images were obtained. As a result of the works conducted, a photo plan was made, with the detail scale of 16 pixels/cm. The performed statistical calcu-

lations based on 14 ground control points showed the accuracy of the geographic grid to be 17 m. The detailed description of the methodology of the photography and of data processing, as well as the photo plan itself, are given in [*Pryakhin et al., 2015*].

GPR sounding was performed using the equipment of GSSI (Geophysical Survey Systems Inc., USA) SIR-3000 simultaneously at two frequencies: 270 and 900 MHz. Their technical characteristics are provided in [*GSSI Antennas Manual, 2014*]. As a transport vehicle, a snowmobile was used (Fig. 2, *a*). The survey was conducted at the velocity of 5 km/h. The total length of the routes was about 20 km. The GARMIN GPSmap 60 with a remote antenna GA 25MCX was used for navigation with the accuracy of about 2 m. Before the GPR sounding, equipment tests and methodological testing works were conducted, in order to clarify the possibilities of the available equipment [*Popov and Polyakov, 2016*].

Core drilling was performed with a Kovacs mechanical ice auger (Kovacs Enterprises, USA), which ensured the borehole diameter of 17 cm and the diameter of the core 14 cm (Fig. 2, *b*). Immediately after core sampling, the temperature inside it was measured at different horizons, followed by description of the core samples, their photography and sawing them into slabs, with their density determined, too.

The density of the core slabs was identified as the ratio between their mass and volume. For this purpose, the samples were weighed on the Fisherman OCS20K electronic scale (China) with the accuracy of ±20 g. The core slabs had the average weight of 2 kg and a shape which was very close to cylindrical. Their volume was determined by the trigonometric method. The error of determining the core slab volume, based on the characteristics of the equipment accuracy and the measurement method, was evaluated to be 6 %.

The ice temperature was determined with a portable electronic thermometer GTH 175/MO (Germany) for measuring snow and ice temperature with the operating range from –199 to +199 °C and the accuracy of ±0.1 °C. At the previously established points for core sampling, an opening was drilled about 6 cm deep, so that the thermometer probe could be completely immersed into it (Fig. 2, *c*). Then some time was allowed (usually up to 2 minutes), for the probe temperature to become equal to the core temperature, after which measurement was made.
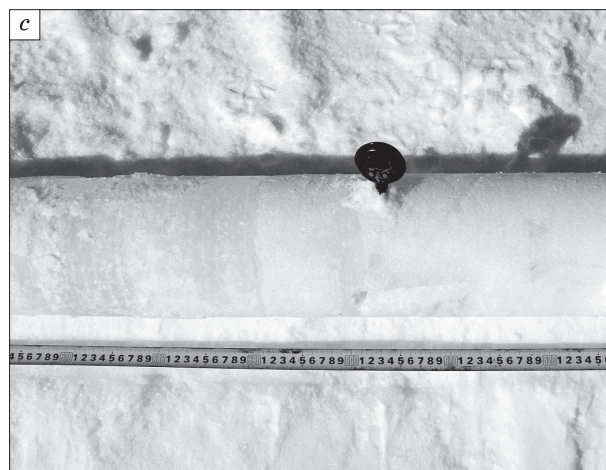

Fig. 2. GPR profiling (*a*), core drilling (*b*) and core temperature measurement (*c*).

The photos were provided by S.S. Pryakhin, January 2015.

69

THE RESULTS
OF ICE CORE SAMPLING

Five ice core samples were selected during the GPR sounding in the territory of the survey (Fig. 3) in the points with the following coordinates: 66°33.810′ S, 93°00.764′ E (borehole 1); 66°34.154′ S, 93°01.143′ E (borehole 2); 66°34.507′ S, 93°01.778′ E (borehole 3); 66°33.863′ S, 93°00.550′ E (borehole 5) and 66°34.307′ S, 93°01.084′ E (borehole 6), to the depths of 405, 525, 625, 330 and 677 cm, respectively (Fig. 1). Their density and temperature profiles are shown in Fig. 4. The stratigraphic description of the cores made in accordance with [*Glaciological Dictionary, 1984*] is shown in Fig. 5.

The snow cover layer accumulated over the winter period during summer reaches the phase transition point and passes a deep stage of constructive metamorphism [*De Quervain, 1966*], with fine-grained snow turning into large-crystal firn with multiple ice inclusions. In accordance with the international classification of glaciers [*Paterson, 1984*], this region may be referred to the infiltration zone.

At the drilling point 6 (Fig. 1) a unique behavior of the temperature profile in the glacier pack was discovered. Although at the depth of 4 m the temperature dropped to −5 °C, at the depth of 6.4 m it rose to the phase transition point (Fig. 4, *b*), i.e., water was discovered at the given horizon. Tentatively, this phenomenon may be attributed to the presence of actively formed unhealed crevasses and micro-crevasses, through which thawed water penetrates from the sur-
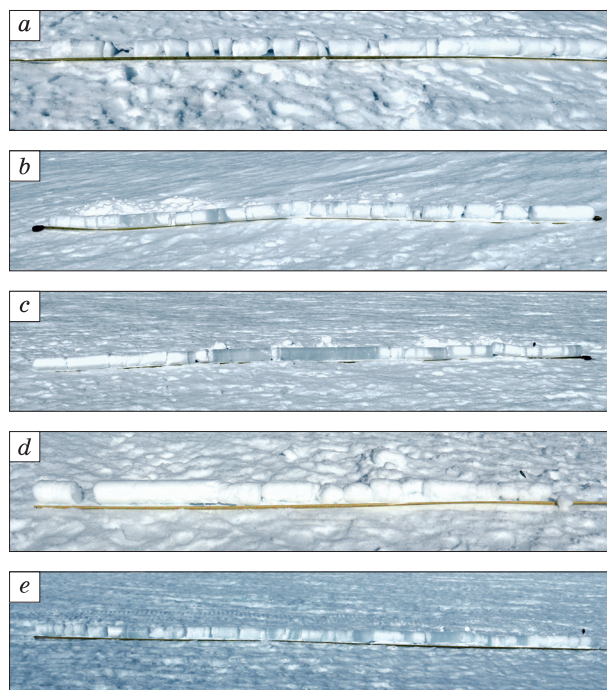

Fig. 3. Photos of core samples: core sample 1 (*a*), core sample 2 (*b*), core sample 3 (*c*), core sample 5 (*d*), core sample 6 (*e*).
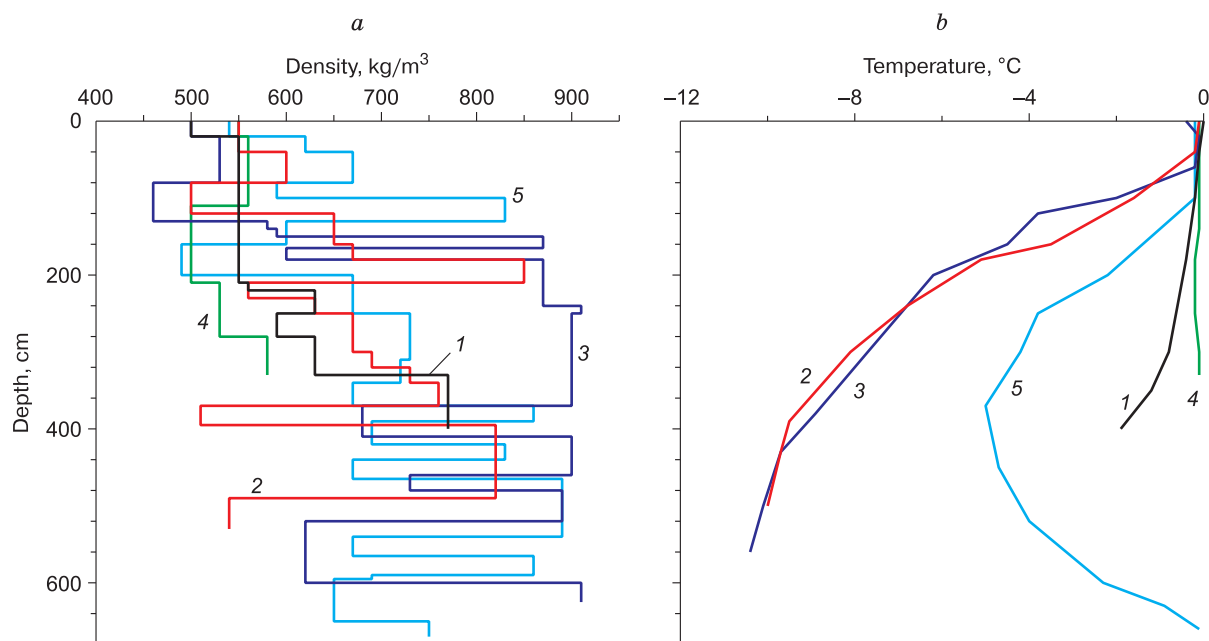
The photos were provided by S.S. Pryakhin, January 2015.

face into the snow and firm layer to the level of the beginning of meteoric ice.

Fig. 4. Density (*a*) and temperature (*b*) profiles in accordance with core data:

1 – core sample 1; *2* – core sample 2; *3* – core sample 3; *4* – core sample 5; *5* – core sample 6.
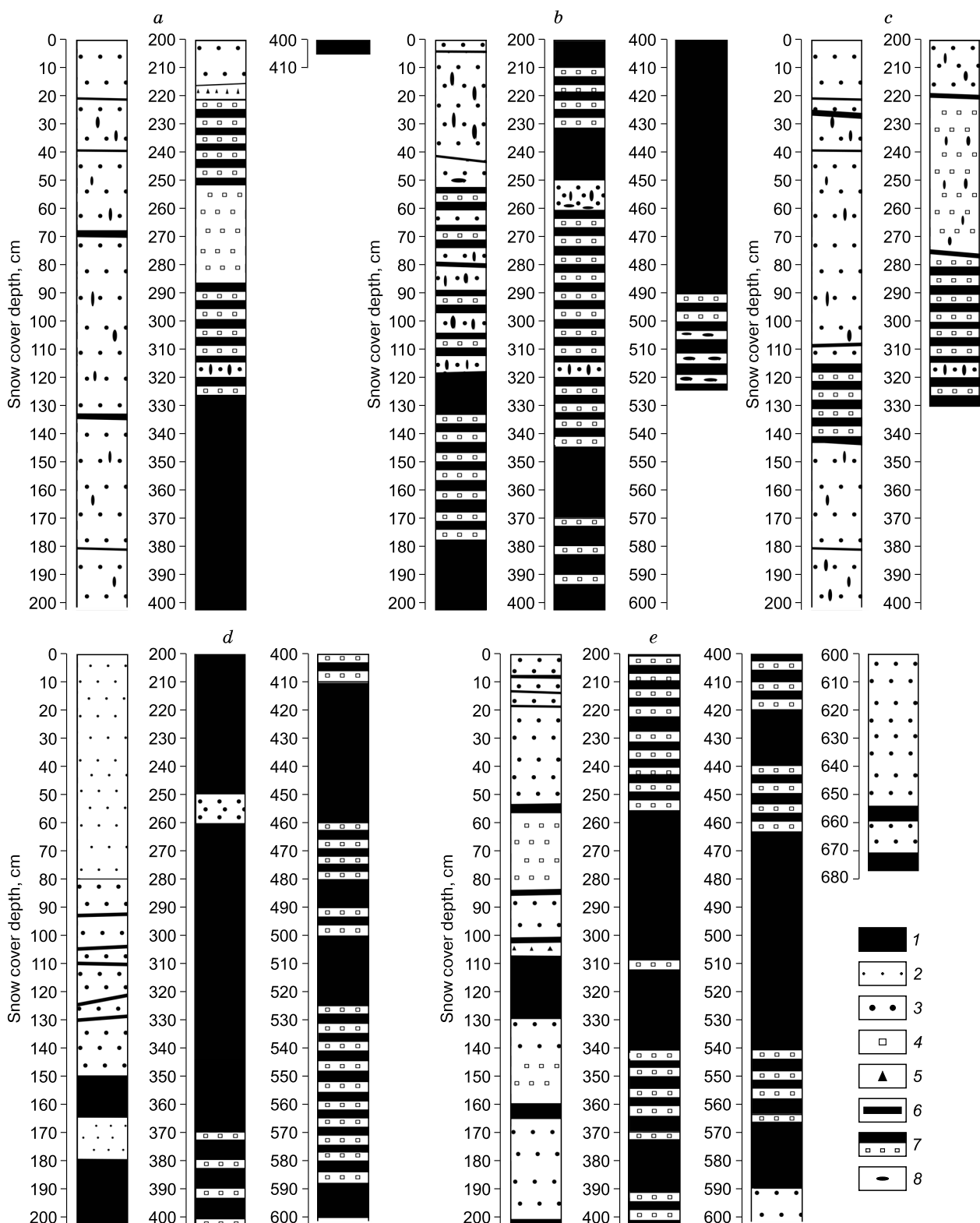
Fig. 5. The stratigraphic description of the core samples: core sample 1 (*a*), core sample 2 (*b*), core sample 5 (*c*), core sample 3 (*d*), core sample 6 (*e*).

1 – glacier ice; *2* – fine and medium-grain snow; *3* – large-grain snow or firn; *4* – edged crystals; *5* – deep hoar-frost; *6* – ice crust; *7* – glacier ice with inclusions of edged crystals; *8* – ice inclusions.

COMPARISON OF GPR
AND ICE CORE DATA

The GPR survey was conducted based on a system of control, tie and diagonal lines 20 km in total length (Fig. 1). Practically all of them were carried out in sounding simultaneously at two frequencies 270 and 900 MHz. Insignificant incidents when technical failures took place, were an exception to this rule. Availability of two such different frequencies allowed, on the one hand, quality data relating to be obtained at the depths of several dozen meters and, on the other hand, the specific features of the structure of the surface part of the glacier to be clarified. The latter was very important for identification and the study of crevasses.

The radar sounding data were processed in accordance with the standard methodology. It included: 1) connecting individual fragments into one profile; 2) conjunction of each sounding point in the plan; 3) all-round checking of the plan conjunction data; 4) improvement of the contrast of the boundaries targeted (filtration, non-linear amplification); 5) selecting parameters of visualization of the temporary transverse sections (the color gamut, etc.); 6) selecting the velocity model of the medium; 7) digitalization of the targeted boundaries; 8) calculation of the closing errors in the route crossing points and their statistical processing; 9) final visualization of data and making a complete set of maps. This calculation method has proven to work well in processing of radio echo and geo radar data obtained in Antarctica over many years. For an unknown reason, the input data are characterized by the presence of intense noise observed in the time-sections as horizontal strips when sounding at the frequency of 270 MHz. In certain cases, they fully or partially mask the tar-

get boundaries and thus prevent successful interpretation of the material without preliminary processing. Horizontal filtration is an effective tool of combatting it. As applied to the available data, the positive results were achieved by using a sliding window 200 routes wide.

The ice cover of the region under study is characterized by a rather complicated structure, which is confirmed by the core sampling data (Figs. 3 and 5). This seems to be related to climatic conditions: high temperatures in the summer period ensure intense surface ice melting and filling of crevasses with thawed water, with subsequent penetration into the depth of the glacier.

Shown in Fig. 6 is a GPR time-section for route MR17-56a of the southeastern direction, which can be used, in a certain sense, to characterize the glacial structure of the entire region under study. Besides, it begins in the immediate vicinity of borehole 3 and ends near borehole 1, thus allowing comparison of glaciological and GPR data.

Low reflection *1* was recorded in the section, formed by a direct wave and corresponding to the position of the snow surface (Fig. 6). Its low intensity was caused by the use of filtration, which resulted in suppression of all the extended horizontal boundaries. High-contrast reflection *2* is of interest, too. If we reject clearly improbable variants, then, judging by the intensity and shape, it may be related to the presence of the aqueous layer. As a matter of fact, this is the appearance of reflection from subglacial lakes in the radio-echo time-sections collected previously [*Popov, 2010; Popov and Chernoglazov, 2011; Wright and Siegert, 2011; Popov and Popkov, 2015*]. This is confirmed by the data provided by the thermometric evaluation of borehole 1 (Fig. 4, *b*).
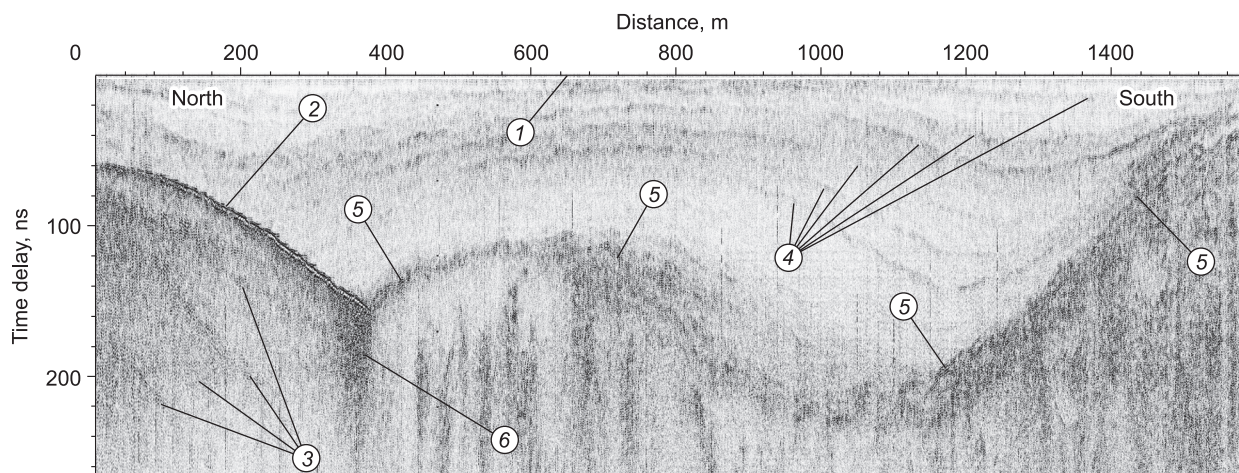

Fig. 6. GPR time-section for route MR17-56a.

1 – direct wave; *2* – reflection related to the presence of a water layer and being a borderline between the snow-firn layer and meteoric ice; *3* – layers inside the meteoric ice; *4* – layers forming the snow-firn layer; *5* – the borderline between the snow-firn layer and meteoric ice; *6* – meteoric ice formed by penetration of thawed water.

Below reflection *2* there are intense reflections *3*, which at times (in particular, at neighboring routes) cross reflections *2* and continue into the above medium by rather intense layers *4*. This means that reflection *2* is related to a rather thin layer of fresh melted water. This, in its turn, indicates that reflection *2* is likely to separate also the relatively loose snow-firn layer from consolidated glacier ice, which, being considered practically impermeable [*Glazovsky and Macheret, 2014*], is a natural obstacle for thawed water. This mechanism has been described in detail in [*Glazovsky and Macheret, 2014*].

From the beginning of the route, at the distance of 380 m, the water-bearing layer ends, and contrast clearly defined borderline *2* becomes the vague and more voluminous borderline *5*. The contrast wedge-shaped area *6*, located at the junction of borderlines *2* and *5*, seems to result from penetration of thawed water into the depth of the glacier by micro crevasses or otherwise. However, judging by the character of the reflection and by the absence of distortions of the below located borderlines, region *6* is frozen, rather than thawed, water.

Thus, if our arguments are correct, reflections *2* and *5* with a high degree of probability mark the borderline between the snow-firn layer and the glacier ice. There are two possibilities to test this: to analyze the core sample and to determine the propagation velocity of electromagnetic waves in the layers above and below this borderline.

In the area of boreholes 1 and 3, the reflections discussed are located at time delays 61 and 40 ns, respectively, i.e., at the depths of 7.5 and 5.0 m, with the lowest out of the reasonable values of permittivity of the snow-firn layer (1.5). However, due to organizational challenges, we were able to obtain the core samples only from the depths of 405 and 625 cm, respectively.

Consider the data on core 1 (Fig. 3, *a*). In accordance with the density profile (Fig. 4, *a*) and the stratigraphic description (Fig. 5, *a*), ice with inclusions of crystals and with density of 770 kg/m^3 begins at the depth of 330 cm (solid ice is characterized by density exceeding 800 kg/m^3 [*Glaciological Dictionary, 1984*]). Above is the snow-firn layer. However, according to the range of reasonable permittivity values, borderline *2* cannot be at such a small depth. It is likely that one of borderlines *4* corresponds to it, and denser solid ice is located much lower.

Consider core sample 3 (Fig. 3, *c*), solid ice, with density of about 900 kg/m^3, begins from the depth of 250 cm. However, below 370 cm its density begins to vary much, which seems to be related to inclusions of large-grain firn, violating solidity of the ice. In accordance with the GPR data collected in the immediate vicinity of the borehole, we may assume that borderline *5* corresponds to the depth of 370 cm. In the area

of the section located above reflection *5*, there are no reflections (i.e., the medium is homogeneous), while below it they are numerous (the medium is heterogeneous). If our assumption is correct, the permittivity of the snow-firn layer located above borderline *5* is about 2.7, which is quite an acceptable value.

THE KINEMATIC MODEL OF THE MEDIUM CALCULATED BY THE TRAVEL-TIME CURVES OF DIFFRACTED WAVES

Inhomogeneities in the mass of the glacier are formed by diffracted waves. Based on their travel-time curves, one can develop quite a good kinematic (permittivity) model of the medium, which will allow recalculation of the GPR time-section into a depth-section [*Popov, 2002; Vladov and Starovoitov, 2004; Macheret, 2006; Glazovsky and Macheret, 2014*]. Due to their extension and depth, crevasses are in most cases excellent reflectors; therefore, they form numerous and rather intense diffracted waves with centers located at different depths [*Glazovsky and Macheret, 2014; Popov and Eberlein, 2014; Popov and Polyakov, 2016*]. This, in its turn, will allow the required amount of statistical data to be obtained, to improve the accuracy of the kinematic model. It would be fair to state that in a number of cases this statement is not exactly correct. In [*Popov and Polyakov, 2016*] it is shown that the crevasses formed in the snow-firn layer are marked in the GPR time-section by significant attenuation of the signal and do not generate intense reflections. In the area under study, these objects are formed in glacier ice and, according to the authors' observations, have rather even, almost vertical, walls. This results in the fact that they are marked by rather intense diffracted waves.

To develop a kinematic model, 56 travel-time curves of diffracted waves, the diffraction points of which were located above boundaries *2* and *5* (Fig. 6), were calculated. In some cases, we were able to make several measurements at different depths in one point; then the values within one layer were averaged. Characteristic diffracted waves used for calculations are shown in Fig. 7. The position of the measurement points is shown in Fig. 8. Calculations for the upper layer were made based on the assumption regarding its homogeneity and isotropic character [*Popov, 2002*]. Calculations for the lower region were made within the framework of a model for inclined-layered medium.

Based on the calculation results, a schematic of permittivity of the upper layer was composed (Fig. 8). The data obtained indicate that this value varies from 1.43 to 3.08. The lowest values of permittivity correspond to snow cover with the lowest snow density [*Robin, 1975*]. They were observed in the central and eastern parts of the region of works. Around its periphery, there are regions with higher values of per-
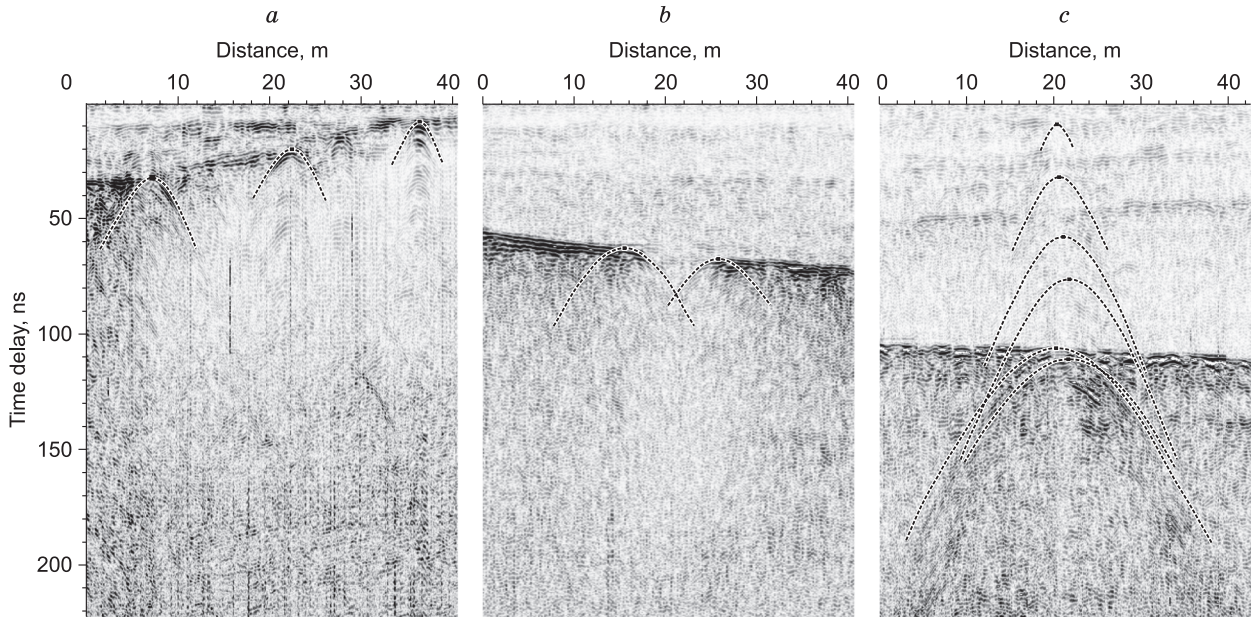
Fig. 7. Fragments of GPR time-sections with diffracted waves accepted for calculation of permittivity.

Diffracted waves caused by: *a* – narrow crevasses; *b* – edge parts of the crevasse on the inner glacial layer; *c* – a deep and voluminous crevasse. The theoretical travel-time curves are shown by dashed lines.

mittivity and hence with higher densities. This is in good agreement with the authors' observations.

Evaluate the error of determining permittivity ε:

$$\varepsilon = \frac{c}{2x}\sqrt{\tau^2 - \tau_0^2},$$

where x is the distance along the horizontal axis between the diffraction point and a certain value on the branch of the travel-time curve; τ_0 is the delay of the reflected signal in the diffraction point; τ is the delay of the reflected signal in the considered point of the travel-time curve; c is the propagation velocity of electromagnetic waves in vacuum [*Popov, 2002*].

In accordance with the error theory, the relative error is the following:

$$\frac{\delta\varepsilon}{\varepsilon} = \sqrt{\left(\frac{\delta x}{x}\right)^2 + \left(\frac{\delta\tau}{\tau}\right)^2}. \qquad (1)$$

Evaluate the addends under the radical sign in (1). The precision of the distance δx, in accordance with the site observations, is about 2 m. The characteristic length of the branches of the travel-time curve is about 5–7 m (Fig. 7). The second addend in (1), i.e., the square of the relative error of determining the delay, is much less than the first one. Therefore, it may be neglected. Thus, the error of determining the permittivity of the upper layer is about 30 %. It may be reduced only by raising the accuracy of the distance, i.e., by carrying out a series of specific studies.

Taking into account such high error values, we will consider the upper layer as homogeneous and isotropic. As an effective value of permittivity, we take the averaged value of the schematic (Fig. 8) to be equal to 2.13 (the propagation velocity of electromagnetic waves is 205.6 m/μs), which corresponds to the firn layer [*Macheret, 2006*].

At the GPR time-sections, many intense diffracted waves are recorded, the diffraction points of which are below the snow-firn layer (Fig. 7, *c*). Using the model of the inclined-layered medium, 77 such travel-time curves were calculated. As previously, we were able to make several measurements in one point at different depths at times. In this case, the values were averaged within one layer. The positions of the measurement points are shown in Fig. 8. The inset for the figure shows a histogram of the permittivity profiles. In accordance with the results of statistical processing, the mean permittivity of this medium is 3.0 (the propagation velocity of electromagnetic waves is 173.2 m/μs). This value is very close to the classical value for ice [*Macheret, 2006*].

Thus, reflections *2* and *5* (Fig. 6) mark the interface between the snow-firn layer and meteoric ice. Shown in Fig. 9 is the schematic of the depth of the snow-firn layer of the district under study. The map contours are somewhat less than the territory of the survey. This is related to the fact that we were not able to mark the borderline for all the routes. As it follows from Fig. 9, the thickness of the snow-firn layer increases in the eastern direction.
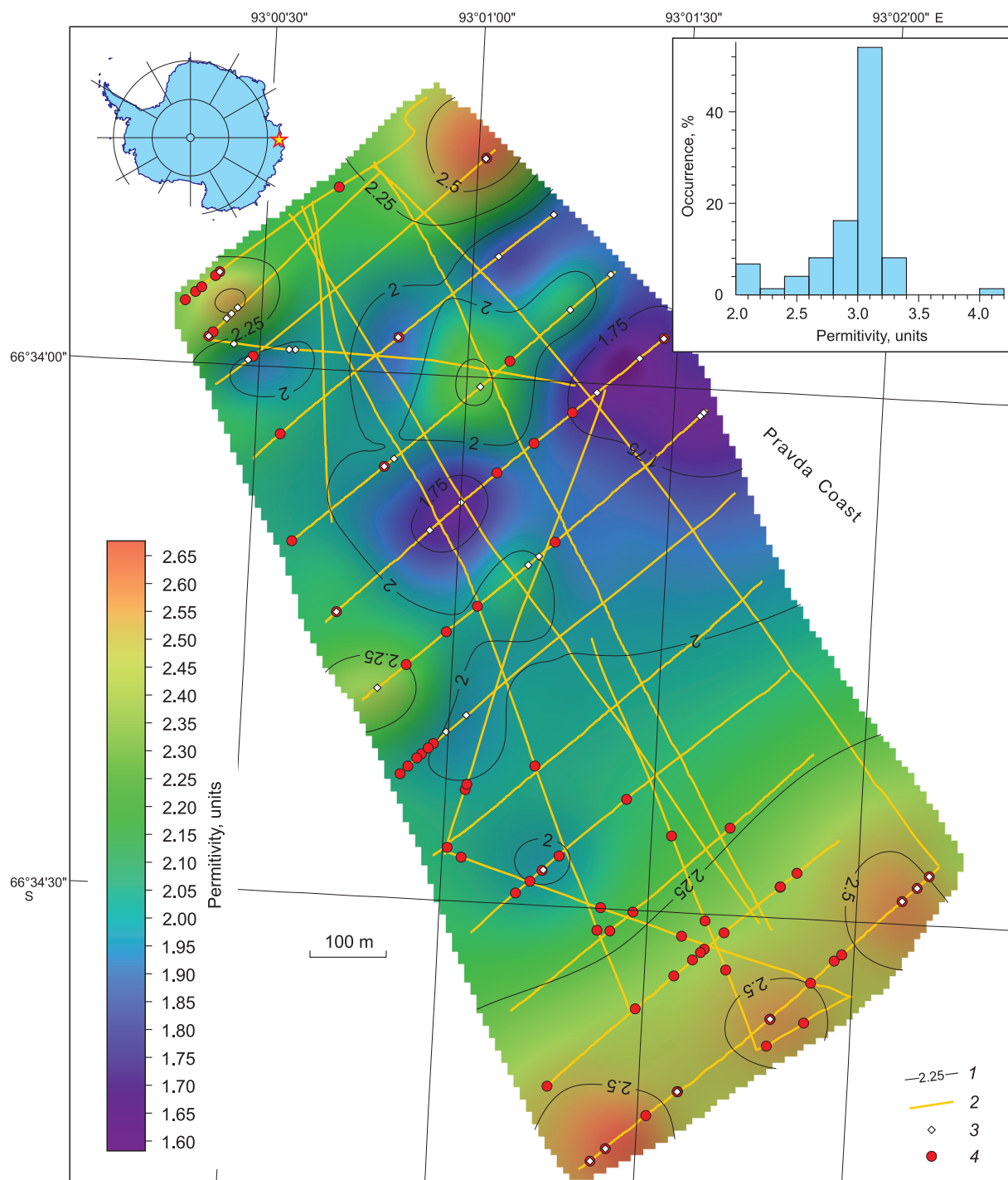
Fig. 8. Permittivity of the snow-firn layer determined by the travel-time curves of diffracted waves.

1 – contour lines and their values; *2* – GPR routes; *3* – position of the diffracting points of the travel-time curves accepted for processing and located in the snow-firn layer; *4* – position of the diffracting points of travel-time curves accepted for processing and located in the meteoric ice layer. Inset: a histogram of permittivity profiles of the ice layer determined by the travel-time curves of diffracted waves.
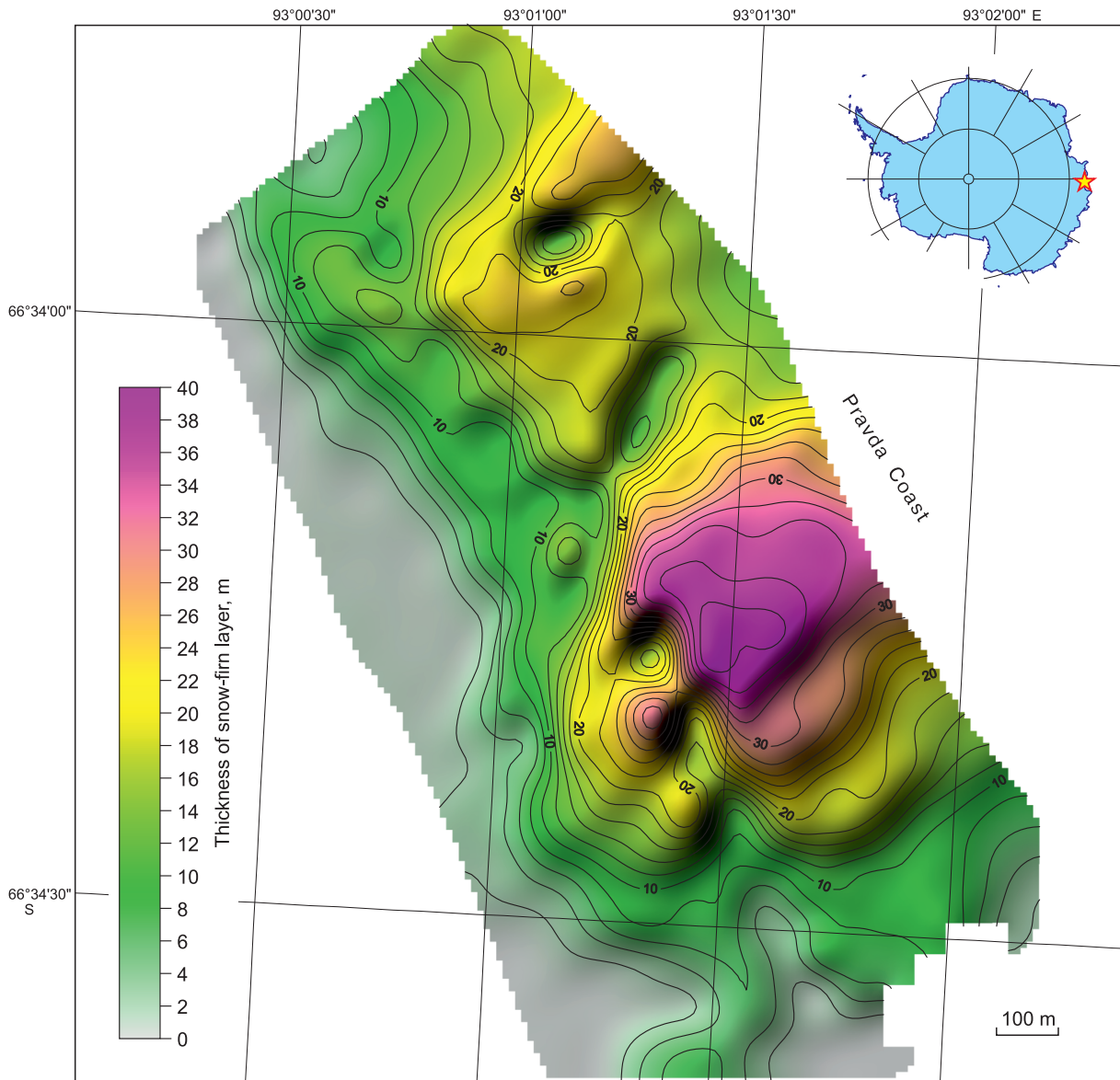
Fig. 9. Thickness of the snow-firn layer in the region under study.

CONCLUSION

In the season of the 60th RAE, large-scale comprehensive glacio-geophysical observations were conducted in the area of the Mirny station, the results of which have only started to be published. It was found out in the course of the works that there is a water saturated layer in the northern part of the glacier at the depth of about 6 meters. The authors believe that it is related to the presence of crevasses, through which melted water penetrates from the surface and becomes accumulated on the border between the snow-firn layer and the meteoric ice. Then, in the southern direction, this layer disappears at the distance of about 380 m from the northern part of the survey territory. The GPR data allowed use to reveal the borderline between the snow-firn layer and meteoric ice. In addition, due to the presence of numerous crevasses, which are natural reflectors and form diffracted waves, the authors were able to evaluate the permittivity of the snow-firn layer. Analyzing the travel-time curves, we found out that the permittivity varied from 1.43 to 3.08, with the average value being 2.13. The thickness of the snow-firn layer is several dozens of meters. In a similar way, permittivity of meteoric ice was evaluated in this area. It totaled 3.0.

Design and construction of runways for ice airfields are difficult tasks. Along with geometric factors presented in the official Russian national and interna-

tional papers regulatory documents (Guidelines on Operation of Civil Airfields, Standards of Worthiness for Operation of Airfields, Federal Aviation Regulations-69, Special Construction Standards 3772, etc.), such as the width, length, maximums slope and roughness degrees, it is important to know the structure of the surface part of the glacier. The situation becomes essentially aggravated, if the region is located in the coastal part of Antarctica, for which high glacier flow velocities and the resulting near-surface crevasses are characteristic. It is no less important to know the structure of the glacier, if runways are to be formed on sea ice. The erroneous idea of ice cover thickness, the presence of crevasses or the beginning of destructive processes may have extremely detrimental and irreparable effects. GPR profiling is the most effective, reliable and timely method of their identification. As the authors' experience shows, this method allows assessment of such important parameters of the crevasses as their configuration, depth, thickness of the snow or snow-firn bridge over them, as well as indirect assessment of the cover thickness. As applied to sea ice, this method allows rather fast assessment of its structure [*Popov and Polyakov, 2015*], as well as timely identification of the beginning of failure or hummocking.

During the field works, complex engineering ice survey was carried out. Such large scale and comprehensive works aimed at solution of one task had not been conducted in Antarctica for decades.

References

De Quervain, M.R., 1966. On the Metamorphism of Snow. Led i Sneg (Edited by W.D. Kingery). Mir, Moscow, pp. 329–344. (in Russian)

Glaciological Dictionary, 1984. Edited by V.M. Kotlyakov. Gidrometeoizdat, Leningrad, 433 pp. (in Russian)

Glazovsky, A.F., Macheret, Yu.Ya., 2014. Water in glaciers. The methods and results of geophysical and remote survey. GEOS, Moscow, 527 pp. (in Russian)

GSSI Antennas Manual, 2014. Geophysical Survey Systems, Inc., Salem, NH, MN30-903 Rev. E, 99 pp.

Lukin, V.V., Kornilov, N.A., Dmitriyev, N.K., 2006. Soviet and Russian Antarctic expeditions in figures and facts (1955– 2005). Arctic and Antarctic Research Institute, St. Petersburg, 456 pp. (in Russian)

Macheret, Yu.Ya., 2006. Radio Sounding of Glaciers. Nauch. Mir, Moscow, 392 pp. (in Russian)

Paterson, W.S.B., 1984. The Physics of Glaciers. Mir, Moscow, 472 pp. (in Russian)

Polyakov, S.P., Martyanov, V.L., Lukin, V.V., 2015. Snow-ice take off runways of the Russian Antarctic expedition: preparation and development prospects. Ros. Polyar. Issled. 2 (20), 31–35.

Popov, S.V., 2002. Determining the mean velocity of propagation of electromagnetic waves in a glacier by hyperbolic reflections from inhomogenuities, Materialy Glyatsiolog. Issled., Iissue 92, 223–225.

Popov, S.V., 2010. Radio echo sounding of shallow subglacial lakes: the theoretical prerequisites and practical results. Led i Sneg 4 (112), 5–14.

Popov, S.V., Chernoglazov, Yu.B., 2011. Vostok Lake, East Antarctica: shore line and surrounding subglacial water cavities. Led i Sneg 1 (113), 13–24.

Popov, S.V., Eberlein, L., 2014. The experience of using a geo radar to study the structure of the snow-firn layer and ground of East Antarctica. Led i Sneg 4 (128), 95–106.

Popov, S.V., Polyakov, S.P., 2015. The results of glaciological GPR research and methodology works in the area of the Antarctic field base Molodezhnaya in the season of the 60th RAE (2014/15). Probl. Arktiki i Antarktiki 106 (4), 54–62.

Popov, S.V., Polyakov, S.P., 2016. Ground-penetrating radar sounding of the ice crevasses in the area of the Russian Progress and Mirny stations (East Antarctica) during the field season of 2014/15. Earth's Cryosphere (Kriosfera Zemli) XX (1), 82–90.

Popov, S.V., Polyakov, S.P., Pryakhin, S.S., Martyanov, V.L., Lukin, V.L., 2015. Application of the glaciological geophysical methods to ensure safety of logistical operations in Antarctica. Ros. Polar. Issled. 3 (2), 29–31.

Popov, S.V., Popkov, A.M., 2015. Seismic and radio-echo sounding study of the Pionerskoe subglacial lake area, East Antarctica. Earth's Cryosphere (Kriosfera Zemli) XIX (2), 95–99.

Pryakhin, S.S., Popov, S.V., Sandalyuk, N.V., Martyanov, V.L., Polyakov, S.P., 2015. Aerial survey of the regions of the Russian Antarctic research stations Mirny and Progress in the season of 2014/15. Led i Sneg 55 (4), 107–113.

Robin, G. de Q., 1975. Velocity of radio waves in ice by means of interferometric technique. J. Glaciol. 15 (73), 151–159.

Savatyugin, L.M., Preobrazhenskaya, M.A., 1999. Russian Research of Antarctica. Gidrometeoizdat, St. Petersburg, vol. I, 360 pp. (in Russian)

The First continental expedition of 1955–1957. A general description, 1959. Proceedings of the Soviet Antarctic Expeditions, vol. 1, 212 pp.

Treshnikov, A.F., 1963. The history of discovery and exploration of Antarctica. Geografgiz, Moscow, 431 pp. (in Russian)

Vladov, M.L., Starovoitov, A.V., 2004. Introduction to GPR Sounding. Moscow University Publishing House, Moscow, 153 pp. (in Russian)

Wright, A., Siegert, M.J., 2011. The identification and physiographical setting of Antarctic subglacial lakes: an update based on recent geophysical data for Subglacial Antarctic Aquatic Environments, in: Subglacial Antarctic Aquatic Environments. Edited by M. Siegert, C. Kennicutt, B. Bindschadler. Washington DC, AGU Geophys. Monograph 192, pp. 9–26.